Optical spiral waves supported by competing nonlinearities

Stefano Longhi
Istituto Nazionale per la Fisica della Materia, Dipartimento di Fisica, Politecnico di Milano, Piazza L. da Vinci 32, I-20133 Milano, Italy
(Received 5 December 2001; published 5 April 2002)

Four-phase spiral waves are predicted to exist in a nonlinear optical cavity with competing quadratic (i.e., $\chi^{(2)}$) and cubic (i.e., $\chi^{(3)}$) nonlinearities. These spatial structures are found in the mean-field model of a doubly resonant type-II frequency-degenerate optical parametric oscillator with an intracavity $\chi^{(3)}$ isotropic medium. Degenerate four-wave mixing of signal and idler fields induced by the $\chi^{(3)}$ medium breaks the phase invariance of the down-conversion process, producing *nonlinear* phase locking with four possible phase states. A parametrically forced Ginzburg-Landau equation is derived to explain the existence of multiphase spiral waves.

DOI: 10.1103/PhysRevA.65.045802 PACS number(s): 42.65.Sf, 42.65.Yj

The study of spatial-temporal structures of light interacting with nonlinear quadratic media both in traveling-wave configurations and in optical cavities has attracted continuous interest in recent years. Such interest has been mainly motivated, on the one hand, by the possibility of achieving in nonlinear optics a rich ''laboratory'' for the study of the general laws underlying the formation of spatiotemporal structures in spatially extended nonlinear systems. On the other hand, the existence of localized states and spatial multistability in $\chi^{(2)}$-based nonlinear optical devices may be of potential relevance in applications such as all-optical control and processing of light. In the cavityless case, great attention has been devoted to the analysis of $\chi^{(2)}$ cascading processes and to the study of spatial (or temporal) propagative solitons (see, e.g., [1]); in particular, the effects of competing $\chi^{(2)}$ and $\chi^{(3)}$ nonlinearities have been investigated in detail [2]. The inclusion of an optical cavity allows for the formation of dissipative spatial structures. The formation of patterns, domain walls, and localized structures (cavity solitons) in particular has been investigated theoretically for the optical parametric oscillator (OPO) model (see, e.g., [3] and references therein), and the experimental observation of some of these structures has been recently reported [4]. Of particular relevance is the class of phase-locked OPOs, in which the generated signal and idler fields have fixed values for their phase [5,6]. These devices, in addition to being of extreme importance for applications in frequency metrology and quantum optical studies, have attracted some interest also for the study of the spatial-temporal dynamics of multiphase systems [7–15]. In most previously studied phase-locked OPO systems, spatially self-organized structures arise from a *phase bistability* due to degeneracy of the idler and signal waves. Ising-like domain walls that separate two equivalent phase states were predicted earlier for degenerate type-I OPOs [16], and a detailed and comprehensive study of the dynamics of domain walls was recently given in [17]. In [18] it was shown that type-II frequency-degenerate OPOs, in which phase bistability is induced by cavity birefringence, enable a richer dynamics, predicting the existence of Bloch domain walls, the Ising-Bloch transition, and spiraling defects. The occurrence of multistability among $n>2$ different phase states allows for further interesting phenomena, the most notable one being the formation of multiphase spiral waves [9–14]. Such structures generally arise when a spatially extended system near a Hopf biurcation is parametrically forced at a frequency n times the Hopf bifurcation frequency [7]. Although the study of general properties of multiphase spiral waves and patterns has been worked out within normal-form amplitude equations [7,14,15] and interesting phase front instabilities have been predicted and observed in the $n=4$ case [10–12], there are to date very few explicit examples of nonlinear systems displaying $n=3$ or $n=4$ phase multistability, the most notable one being the parametrically forced Belousov-Zhabotinsky reaction system [10–13]. In such systems the occurrence of the phase multistability is artificially realized by periodic modulation of a control parameter. The existence of three-armed spiral waves supported by the bulk nonlinearity of the system, i.e., without the need for periodic modulation of parameters, was recently predicted in nonlinear optics in a special class of nondegenerate self-phase-locked OPOs as a result of a multistep $\chi^{(2)}$ process [19]. Nevertheless, $n=4$ phase multistability seems unlikely in *purely* quadratic optical devices, such as the device considered in [19], and the search for an optical system displaying a dynamical scenario typical of $n=4$ multiphase systems, until now realized solely in a chemical reaction system, appears thus of a certain relevance.

In this Brief Report we investigate theoretically the effects of an isotropic cubic nonlinearity in the process of optical parametric oscillation for a type-II interaction and show that the competing $\chi^{(3)}$ nonlinearity leads to an $n=4$ phase multistability and to the existence of four-phase spiral waves. We consider a doubly resonant type-II OPO in a ring cavity with flat mirrors containing both a birefringent $\chi^{(2)}$ nonlinear crystal, pumped by a nonresonant pump wave at frequency 2ω, and an isotropic $\chi^{(3)}$ nonlinear medium [Fig. 1(a)]. The pump field is assumed to be linearly polarized along, e.g., the extraordinary y axis of the nonlinear crystal, whereas birefringent phase matching and cavity tuning are accomplished for efficient generation of frequency-degenerate (or quasidegenerate) signal and idler fields at frequency ω linearly polarized along the ordinary, x, and extraordinary, y, axes of the crystal, respectively [see Fig. 1(b)]. In the spirit of the mean-field limit, the signal and idler waves suffer small changes after each round-trip propagation, and their envelopes B_1 and B_2 can be taken approximately uniform along the cavity axis

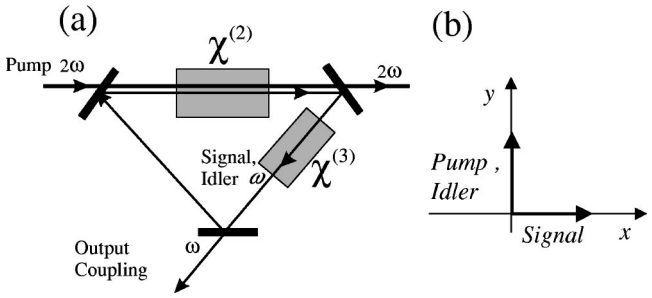

FIG. 1. (a) Schematic of a doubly resonant OPO in a ring cavity with a $\chi^{(3)}$ nonlinearity; (b) type-II phase matching in the birefringent crystal for degenerate down-conversion.

z. The mean-field equation for the intracavity amplitudes B_1 and B_2 then has the general form (see, e.g., [20])

$$\partial_t B_{1,2} = (\Delta B_{1,2}^L + \Delta B_{1,2}^{NL})/T_{1,2}^R, \tag{1}$$

where $\Delta B_{1,2}^L$ and $\Delta B_{1,2}^{NL}$ are the small changes of signal and idler amplitudes in one cavity round-trip due to linear and nonlinear propagation effects, respectively, and $T_{1,2}^R$ are the cavity round-trip times for the two fields. The first term in Eq. (1), $\Delta B_{1,2}^L$, accounts for both cavity effects and diffraction in the paraxial approximation, and reads

$$\Delta B_{1,2}^L = T_{1,2}^R \gamma_{1,2}[-(1+i\Delta_{1,2})B_{1,2} + i a_{1,2}\nabla^2 B_{1,2}], \tag{2}$$

where $\gamma_{1,2}$, $\Delta_{1,2}$, and $a_{1,2}$ are the cavity decay rates, detuning parameters, and diffraction coefficients for the two fields, respectively, defined as in Ref. [21]. The second term in Eq. (1), $\Delta B_{1,2}^{NL}$, comprises the changes of signal and idler waves due to the nonlinear interaction in both the quadratic and cubic media, i.e., $\Delta B_{1,2}^{NL} = \Delta B_{1,2}^{quadratic} + \Delta B_{1,2}^{cubic}$. The explicit expressions for $\Delta B_{1,2}^{quadratic}$ can be derived by integration of the nonlinear wave equations for signal, idler, and pump waves in the $\chi^{(2)}$ crystal after elimination of the pump field from the dynamics as detailed, e.g., in [20]; one obtains

$$\Delta B_{1,2}^{quadratic} = i\frac{\omega\chi^{(2)}\mathcal{E}_p l}{2n_{1,2}c_0}\frac{\exp(i\Delta k l)-1}{i\Delta k l}B_{2,1}^* - \frac{\omega^2\chi^{(2)2}l^2\rho}{4n_{1,2}n_3 c_0^2}|B_{2,1}|^2 B_{1,2}, \tag{3}$$

where n_1, n_2, and n_3 are the refractive indices of signal, idler, and pump waves in the $\chi^{(2)}$ crystal, respectively; l is the crystal length; $\chi^{(2)}$ is the relevant element of the second-order susceptibility tensor involved in the type-II interaction; $\mathcal{E}_p$ is the electric-field amplitude of the incident plane-wave pump beam; $\Delta k = k_y(2\omega) - k_x(\omega) - k_y(\omega)$ is the residual wave vector mismatch of the parametric interaction; and $\rho = -2\{1/(i\Delta k l) + [\exp(i\Delta k l)-1]/(\Delta k l)^2\}$ is a dimensionless complex coefficient that accounts for saturation and $\chi^{(2)}$ cascading effects ($\rho \to 1$ for $\Delta k l \to 0$; see [20]). Finally, the propagation of the frequency-degenerate signal and idler waves through the $\chi^{(3)}$ medium introduces self-phase modulation, cross-phase modulation, and degenerate four-wave mixing terms in the mean-field equation, which read (see, e.g., [22])

$$\Delta B_{1,2}^{cubic} = i\frac{3\pi\mathcal{L}\chi^{(3)}}{4n_0\lambda}\left[(|B_{1,2}|^2 + \mathcal{A}|B_{2,1}|^2)B_{1,2} + \frac{\mathcal{B}}{2}B_{2,1}^2 B_{1,2}^*\right], \tag{4}$$

where λ is the wavelength (in vacuum) of signal and idler waves; n_0 is the (linear) refractive index of the cubic medium at frequency ω; $\mathcal{L}$ is the length of the cubic medium; $\chi^{(3)} \equiv \chi_{xxxx}^{(3)}$; and $\mathcal{A} = [\chi_{xxyy}^{(3)} + \chi_{xyxy}^{(3)}]/\chi_{xxxx}^{(3)}$ and $\mathcal{B} = 2\chi_{xyyx}^{(3)}/\chi_{xxxx}^{(3)}$ are the Maker-Terhune coefficients for the nonlinear $\chi^{(3)}$ medium ($\mathcal{A} + \mathcal{B}/2 = 1$ for an isotropic medium). Substitution of Eqs. (2)–(4) into Eq. (1) allows one to write the mean-field equations for the intracavity signal and idler waves. After introduction of the normalized envelopes $A_{1,2} \equiv B_{1,2}/q_{1,2}$, where $q_1 = q_2[n_2 T_2^R \gamma_2/(n_1 T_1^R \gamma_1)]^{1/2}$ and $q_2 = (n_1 n_3 \gamma_1 T_1^R \lambda^2)^{1/2}/(\pi\chi^{(2)} l)$, and with a suitable choice of the phase of the pump wave $\mathcal{E}_p$, the mean-field equations can be cast in the following form:

$$\partial_t A_1 = \gamma_1\left[-(1+i\Delta_1)A_1 + i a_1\nabla^2 A_1 + \mu A_2^* - \rho|A_2|^2 A_1 + i\sigma_1\left(\theta|A_1|^2 A_1 + \mathcal{A}|A_2|^2 A_1 + \frac{\mathcal{B}}{2}A_2^2 A_1^*\right)\right], \tag{5a}$$

$$\partial_t A_2 = \gamma_2\left[-(1+i\Delta_2)A_2 + i a_2\nabla^2 A_2 + \mu A_1^* - \rho|A_1|^2 A_2 + i\sigma_2\left(\frac{1}{\theta}|A_2|^2 A_2 + \mathcal{A}|A_1|^2 A_2 + \frac{\mathcal{B}}{2}A_1^2 A_2^*\right)\right], \tag{5b}$$

where

$$\mu = (\pi\chi^{(2)}|\mathcal{E}_p|l)|\sin(\Delta k l)/(\Delta k l)|/[\lambda(\gamma_1\gamma_2 T_1^R T_2^R n_1 n_2)^{1/2}]$$

is the dimensionless parametric gain, $\theta = (n_2 T_2^R \gamma_2)/(n_1 T_1^R \gamma_1)$, and $\sigma_{1,2} \equiv [3n_{1,2}n_3/(4\pi n_0)](\mathcal{L}/l)(\lambda/l)\chi^{(3)}/[\chi^{(2)}]^2$ measures the relative strength of third-order versus second-order nonlinearities. The order of magnitude of $\sigma_{1,2}$ largely depends on material parameters and crystal lengths; for instance, assuming a $\chi^{(2)}$ of the order of 10^{-8} esu, typical values for $\chi^{(3)}/[\chi^{(2)}]^2$ may range from ~ 10 for fast electronic nonlinearities to $\sim 10^3$ for molecular orientation; higher values of $\chi^{(3)}/[\chi^{(2)}]^2$ may be achieved using stronger $\chi^{(3)}$ nonlinearities, such as by exploiting resonant electronic nonlinearities (e.g., excitonic semiconductor nonlinearities), saturated atomic absorption, or semiconductor-doped glasses [22]. For typical experimentally accessible values of l and $\mathcal{L}$ and at near-infrared or visible wavelengths, the dimensionless parameters $\sigma_{1,2}$ may hence reach values of the order of ~ 0.1–1 or even higher. The values of $\mathcal{A}$ and $\mathcal{B}$ are determined by the nature of the isotropic nonlinearity; for instance, for the Kerr effect due to off-resonance fast electronic

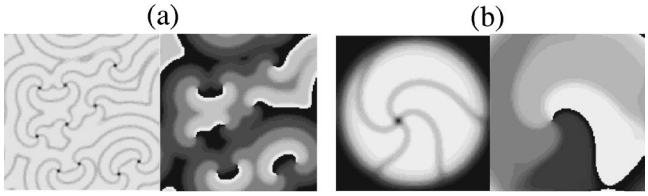

FIG. 2. Rotating four-phase spiral waves obtained from numerical simulations of Eq. (1), from initial noise conditions, for a plane-wave pump (a) and for a super-Gaussian pump (b). The figures show the intensity (left side) and phase (right side) of the signal field at times $t=6000$. Parameter values are $\mu=1.8$, $\sigma_1=0.4$, $\Delta kl=0$, $\Delta_1=1$, $\Delta_2=1.1$, $\mathcal{A}=\mathcal{B}=2/3$ in (a), and $\mu_0=2.7$, $w=44$, $m=4$, $\sigma_1=0.2$, $\Delta kl=-0.1$, $\Delta_1=2$,$\Delta_2=2.2$, $\mathcal{A}=1/4$, $\mathcal{B}=3/2$ in (b). The other parameter values are $\gamma_1=\gamma_2=1$, $a_1=1.05$, $a_2=1$, $\theta=1$, and $\sigma_2=1.1\sigma_1$. In (a) the integration domain is 180×180 wide. A spatial grid of 128×128 points was used; time step $dt=0.02$.

response one has $\mathcal{A}=\mathcal{B}=2/3$, whereas for the Kerr effect in liquids one has $\mathcal{A}=1/4$ and $\mathcal{B}=3/2$ [22].

The zero solution $A_1=A_2=0$ of Eqs. (5), corresponding to the OPO being below threshold, undergoes a Hopf bifurcation with frequency $\omega_c=\gamma_1\gamma_2(\Delta_2-\Delta_1)/(\gamma_1+\gamma_2)$ to a spatially homogeneous state for signal and idler fields at $\mu=\mu_{th}\equiv(1+\Delta^2)^{1/2}$ when $\Delta>0$, where $\Delta\equiv(\gamma_1\Delta_1+\gamma_2\Delta_2)/(\gamma_1+\gamma_2)$ is the effective detuning parameter [21]. In the absence of the competing $\chi^{(3)}$ nonlinearity, Eqs. (5) are invariant under the phase transformation $A_1\rightarrow A_1\exp(i\phi)$, $A_2\rightarrow A_2\exp(-i\phi)$, and phase locking is not possible. The inclusion of the $\chi^{(3)}$ medium breaks the phase invariance and may lead to phase locking of the homogeneous state. Analytical expressions for the homogeneous phase-locked states and domain of existence cannot be derived in a closed form; a simple inspection of Eqs. (5) nevertheless reveals that the phase-locking mechanism, induced by the $\mathcal{B}$-resonant cubic term, is nonlinear and produces a *phase* multiplicity of the uniform state with *four* allowed phases shifted by $\pi/2$ with respect to one another. It should be noted that the $\mathcal{B}$ term of cubic nonlinearity is resonant when signal and idler fields are close to frequency degeneracy, so that phase locking is effective when the Hopf frequency ω_c at the linear instability is close to zero, i.e., for $\Delta_1\simeq\Delta_2$. For $\mu>\mu_{th}$, homogeneous states with different phases, connected by domain walls, may grow and emerge in different spatial regions. We performed a numerical analysis of Eqs. (5) using a pseudospectral split-step technique to study the phase-locking regime for $\Delta>0$ and the dynamics of domain walls above threshold. Starting from the zero solution with a small random noise, shrinking or expansion of different phase domains may be observed after the linear growth, leading to one dominant final phase state; however, more complex dynamical behaviors can be observed. In particular, dynamical states corresponding to four-armed rotating spirals composed of four-phase domains coalescing at one point and rotating around it are possible. Spiral waves are observed using both a plane-wave pump with periodic boundary conditions [see Fig. 2(a)], and a super-Gaussian pump $\mu=\mu_0\exp[-(r/w)^{2m}]$ with radial symmetry [see Fig. 2(b)]. Spirals with different ordered phase states rotate in opposite directions; annihilation of spirals may occur; however, long-lived bound states of counterrotating spirals may be observed. As an example, a stable bound state for a super-Gaussian pump is shown in Fig. 3(a). The tendency to spiraling for domain walls turns out to be very sensitive to the value of cavity detuning imbalance $\Delta_2-\Delta_1$ and strength $\sigma_{1,2}$ of the competing nonlinearity. Although a detailed analysis of dynamical behaviors in parameter space goes beyond the scope of the present work, we nevertheless notice that large-scale numerical simulations indicate that four-phase spirals can be observed under a wide variety of operational conditions. For instance, if we consider parameter values as in Fig. 2(b), spirals are observed for σ_1 varying between ~0.12 and ~0.5; at larger values of competing nonlinearity large spirals and target patterns are typically observed [see Figs. 3(b) and 3(c), respectively], with the appearance of turbulent structures at even higher values of nonlinearity. We also notice that spiral waves may be observed for either off-resonance electronic nonlinearities [Fig. 2(a)] or for cubic nonlinearities due to molecular orientation [Figs. 2(b) and 3].

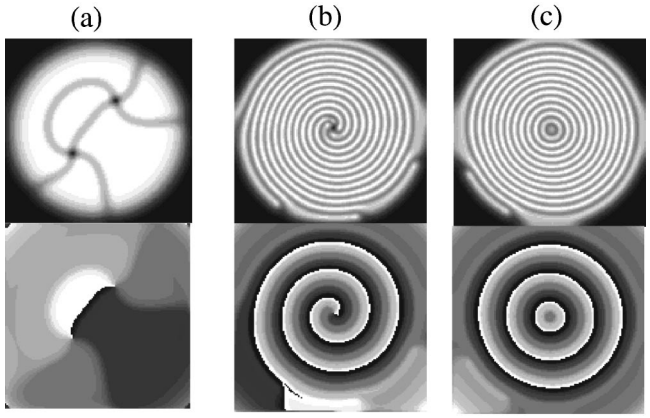

FIG. 3. (a) Bound state of counterrotating spirals. Parameter values are the same as in Fig. 2(b); the stability of the bound state was checked up to time $t=20\,000$. (b) and (c) formation of large rotating spirals and target patterns from small random noise for $\sigma_1=0.6$ [the other parameter values are the same as in Fig. 2(b)].

In order to get some analytical insights into the existence of multiphase spirals and to understand the role of the isotropic cubic nonlinearity, we derived an order parameter equation close to threshold for $\Delta>0$ by a weakly nonlinear analysis of Eqs. (5). By setting $\mu=\mu_{th}+\epsilon^2$, where the smallness parameter ϵ measures the distance from the bifurcation point μ_{th}, and assuming $\omega_c\sim O(\epsilon^2)$ to allow for phase locking, the amplitude equation can be derived as a solvability condition in a multiple-scale asymptotic expansion by an extension of the analysis described in [21,23]. At leading order, one finds that $(A_1,A_2)^T=(1,(1-i\Delta)/\mu_{th})^T\psi(x,y,t)+O(\epsilon^2)$, where the amplitude $\psi\sim\epsilon$ satisfies the following equation:

$$\partial_t\psi=c_1\psi+c_2\nabla^2\psi-c_3|\psi|^2\psi-c_4\psi^{*3}, \tag{6}$$

where we have set

$$c_1=\gamma_1\gamma_2\frac{2\mu_{th}(\mu-\mu_{th})+i(\Delta_2-\Delta_1)(1+i\Delta)}{\gamma_1+\gamma_2+i(\gamma_1-\gamma_2)\Delta}, \tag{7a}$$

$$c_2=\frac{i\gamma_1\gamma_2[a_1-a_2-i\Delta(a_1+a_2)]}{\gamma_1+\gamma_2+i(\gamma_1-\gamma_2)\Delta}, \tag{7b}$$

$$c_3=\gamma_1\gamma_2\frac{2\mathrm{Re}(\rho)+2\Delta\mathrm{Im}(\rho)+i\sigma_2(1+i\Delta)(\mathcal{A}+1/\theta)-i\sigma_1(1-i\Delta)(\mathcal{A}+\theta)}{\gamma_1+\gamma_2+i(\gamma_1-\gamma_2)\Delta}, \tag{7c}$$

$$c_4=\frac{\mathcal{B}\gamma_1\gamma_2}{2}\sqrt{\frac{(\sigma_2-\sigma_1)^2+\Delta^2(\sigma_2+\sigma_1)^2}{(\gamma_1+\gamma_2)^2+\Delta^2(\gamma_1-\gamma_2)^2}}. \tag{7d}$$

The amplitude equation (6) is a parametrically forced Ginzburg-Landau equation that describes quite generally the nonlinear dynamics of a spatially extended system close to a Hopf bifurcation under periodic modulation of parameters [7]. The existence and stability of four-phase spiral waves for such a model equation has been extensively studied in [7,10,11]. It is remarkable that in our optical system these structures are spontaneously supported by the bulk nonlinearity of the system, without the need for temporal modulation of parameters. Finally, it is important to point out that the $n=4$ phase multistability arises due to frequency-degenerate four-wave mixing of signal and idler waves in the isotropic $\chi^{(3)}$ medium [see the last term in Eq. (4)], not from self-phase or cross-phase modulation terms. This means that the existence of four-phase spirals requires a ''true'' cubic nonlinear medium, not an equivalent third-order nonlinearity induced by, e.g., $\chi^{(2)}$ cascading effects. For this reason four-phase spirals seem unlikely in purely quadratic media, although $n=3$ phase multistability is possible in some special cases [19].

In conclusion, four-phase rotating spiral waves have been predicted to exist in a nonlinear optical system with broken phase invariance. These structures have been found in a type-II frequency-degenerate OPO and supported by a competing $\chi^{(3)}$ nonlinearity. The optical system considered in the present work provides one of the few explicit examples of dynamical systems supporting four-phase spiral waves, and hence seems of particular relevance also beyond the field of nonlinear optics.

[1] G. I. Stegeman, D. J. Hagan, and L. Torner, Opt. Quantum Electron. **28**, 1691 (1996); L. Torner and G. I. Stegeman, Opt. Photonics News **12(6)**, 36 (2001).

[2] A. V. Buryak, Y. S. Kivshar, and S. Trillo, Opt. Lett. **20**, 1961 (1995); O. Bang, Y. S. Kivshar, A. V. Buryak, A. De Rossi, and S. Trillo, Phys. Rev. E **58**, 5057 (1998).

[3] G.-L. Oppo, M. Brambilla, and L. A. Lugiato, Phys. Rev. A **49**, 2028 (1994); G. J. de Valcarcel, K. Staliunas, E. Roldan, and V. J. Sanchez-Morcillo, *ibid.* **54**, 1609 (1996); K. Staliunas and V. J. Sanchez-Morcillo, *ibid.* **57**, 1454 (1998); G.-L. Oppo, A. J. Scroggie, and W. J. Firth, J. Opt. B: Quantum Semiclassical Opt. **1**, 133 (1999); M. Le Berre, D. Leduc, E. Ressayre, and A. Tallet, *ibid.* **1**, 153 (1999).

[4] V. B. Taranenko, K. Staliunas, and C. O. Weiss, Phys. Rev. Lett. **81**, 2236 (1998); M. Vaupel, A. Maitre, and C. Fabre, *ibid.* **83**, 5278 (1999); S. Ducci, N. Treps, A. Maitre, and C. Fabre, Phys. Rev. A **64**, 023803 (2001).

[5] E. J. Mason and N. C. Wong, Opt. Lett. **23**, 1733 (1998); C. Fabre, E. J. Mason, and N. C. Wong, Opt. Commun. **170**, 299 (1999).

[6] A. Douillet and J.-J. Zondy, Opt. Lett. **23**, 1259 (1998); J. J. Zondy, A. Tallet, E. Ressayre, and M. LeBerre, Phys. Rev. A **63**, 023814 (2001).

[7] P. Coullet and K. Emilsson, Physica D **61**, 119 (1992).

[8] L. S. Tsimring and I. S. Aranson, Phys. Rev. Lett. **79**, 213 (1997).

[9] V. Petrov, Q. Ouyang, and H. L. Swinney, Nature (London) **388**, 655 (1997).

[10] C. Elphick, A. Hagberg, and E. Meron, Phys. Rev. Lett. **80**, 5007 (1998).

[11] C. Elphick, A. Hagberg, and E. Meron, Phys. Rev. E **59**, 5285 (1999).

[12] A. L. Lin, A. Hagberg, A. Ardelea, M. Bertram, H. L. Swinney, and E. Meron, Phys. Rev. E **62**, 3790 (2000).

[13] A. L. Lin, M. Bertram, K. Martinez, H. L. Swinney, A. Ardelea, and G. F. Carey, Phys. Rev. Lett. **84**, 4240 (2000).

[14] R. Gallego, D. Walgraef, M. San Miguel, and R. Toral, Phys. Rev. E **64**, 056218 (2001).

[15] H.-K. Park, Phys. Rev. Lett. **86**, 1130 (2001).

[16] S. Trillo, M. Haeltermann, and A. Sheppard, Opt. Lett. **22**, 970 (1997); S. Longhi, Phys. Scr. **57**, 611 (1997).

[17] G.-L. Oppo, A. J. Scroggie, and W. J. Firth, Phys. Rev. E **63**, 066209 (2001).

[18] G. Izus, M. San Miguel, and M. Santagiustina, Opt. Lett. **25**, 1454 (2000).

[19] S. Longhi, Phys. Rev. E **63**, 055202 (2001); Eur. Phys. J. D **17**, 57 (2001).

[20] S. Longhi, J. Mod. Opt. **43**, 1089 (1996); P. Lodahl and M. Saffman, Phys. Rev. A **60**, 3251 (1999).

[21] S. Longhi, Phys. Rev. A **53**, 4488 (1996).

[22] See, for instance, R. W. Boyd, *Nonlinear Optics* (Academic Press, New York, 1992).

[23] Z. H. Musslimani, Physica A **249**, 141 (1998).